

Emergent State-Dependent Gravity from Local Information Capacity: A Conditional Thermodynamic Derivation with Scheme-Invariant Cosmological Mapping

[clg]¹

¹[TBD Institution(s)]
(Dated: August 27, 2025)

Core hypothesis. Each proper frame carries a finite quantum information capacity. Approaching this bound triggers a *state-dependent response* that preserves causal stitching with neighboring frames. *Kinematics remain GR-like:* we do not alter null geometry used by EM/GW luminosity distances. The response is *dynamical* (weak-field coupling), not kinematical (no extra time dilation beyond GR).

Scope and conditionality. All quantitative claims are conditional on a single working assumption: (A2) the Clausius relation $\delta Q = T \delta S$ with Unruh normalization holds for small, near-vacuum local Rindler wedges (the *safe window*). We prove this relation holds to working order $\mathcal{O}(\ell^4)$ with $\mathcal{O}(\ell^6)$ corrections (Theorem 1). Within this regime we establish an *equivalence principle for modular response* (EPMR): after mutual-information subtraction with *moment-kill*, the ℓ^4 modular coefficient equals the flat-space value at working order, while curvature dressings enter at $\mathcal{O}(\ell^6)$. See Theorem 1 for the working-order statement and error control.

Main outcomes. (i) A microscopic sensitivity β from MI-subtracted modular Hamiltonians in flat-space QFT (Casini–Huerta–Myers balls, Osborn–Petkou normalization); (ii) a once-and-for-all geometric normalization with *continuous-angle invariance* showing only the *product* $\beta f c_{\text{geo}}$ is physical; (iii) a *conditional, scheme-invariant mapping* $\Omega_\Lambda = \beta f c_{\text{geo}}$ for the FRW zero mode; and (iv) a weak-field flux law with a universal geometric prefactor $5/12$, implying $a_0 = (5/12) \Omega_\Lambda^2 c H_0$. We keep the distance sector GR-like ($\alpha_M = 0$ there), and we *enforce* $|d_L^{\text{GW}}/d_L^{\text{EM}} - 1| \leq 5 \times 10^{-3}$.

Consequences. With no cosmological inputs, $\Omega_\Lambda = \beta f c_{\text{geo}} \approx 0.685$ and $a_0 = (5/12) \Omega_\Lambda^2 c H_0$. An *entropic state-action* law ($\Delta S \geq 0$) determines a monotone $\varepsilon(a)$ that modulates the weak-field response $\mu(\varepsilon) = 1/(1 + \eta \varepsilon)$ with $\eta = 5/12$, suppressing growth and yielding $S_8 \simeq 0.788$ (-7.4% vs. Λ CDM), while EM/GW distances remain GR-like. An *illustrative, capped* environment-gated application to a SH0ES-like catalog nudges $H_0 : 73.0 \rightarrow 71.32$ (SN cap only) and to 70.89 (SN+small Cepheid term), trending toward TRGB/Planck without altering null geometry. Explicit falsifiers and hygiene checks are stated.

I. INTRODUCTION: CORE INSIGHT AND CONDITIONAL SCOPE

a. High level summary. We hypothesize that the geometric side of Einstein’s equations exhibits a *local, state-dependent response* because each small spacetime wedge has finite information capacity. As capacity is approached, the Clausius relation enforces a compensating response so adjacent wedges remain causally stitched. *Kinematics (null cones, EM/GW distances) stay GR-like;* all changes are *dynamical* (response strength in weak fields). Jacobson’s horizon thermodynamics is recovered as the stationary-horizon special case. All claims here are conditional on (A2); if (A2) fails, the construction must be revised. Our working-order result is stated as Theorem 1 (App. I).

b. GR limit (distance sector). In the limit of constant information capacity $\nabla_a M^2 = 0$ (equivalently $\alpha_M \rightarrow 0$), the construction collapses to standard GR — recovering Einstein’s equations with $c_T = 1$ and GR light-cone geometry. Throughout we *keep* $\alpha_M = 0$ *in the distance sector* and confine any late-time variation to the growth/response sector (Sec. X).

c. State variable and coupling. We define a dimensionless state variable $\varepsilon(x)$ encoding fractional deviations of local capacity from its vacuum reference and parameterize

$$\frac{\delta G}{G} = -\beta \delta \varepsilon(x), \quad (1)$$

with β calculable from flat-space QFT (Sec. IV). The weak-field response is encoded by

$$\mu(\varepsilon) \equiv \frac{G_{\text{eff}}}{G_N} = \frac{1}{1 + \eta \varepsilon}, \quad \eta = \frac{5}{12}, \quad (2)$$

so $\mu \rightarrow 1$ in strong fields (GR recovery) and $\mu < 1$ in weak fields (gentle dynamical slowdown).

d. Why $\eta = \frac{5}{12}$. The coefficient follows from the same unit–solid–angle Noether normalization used in the FRW zero mode. Coarse-graining the $\nabla \nabla M^2$ terms over the CHM wedge family yields a quasilinear flux law with a universal boundary–segment ratio; the isotropic null contraction contributes $(4/3)$ and the segment geometry contributes $(5/16)$, giving $(4/3) \times (5/16) = 5/12$. Appendix J shows the identical factor fixing the static acceleration scale $a_0 = (5/12) \Omega_\Lambda^2 c H_0$; using the same bookkeeping in the weak-field $\mu(\varepsilon)$ guarantees scheme/angle invariance.

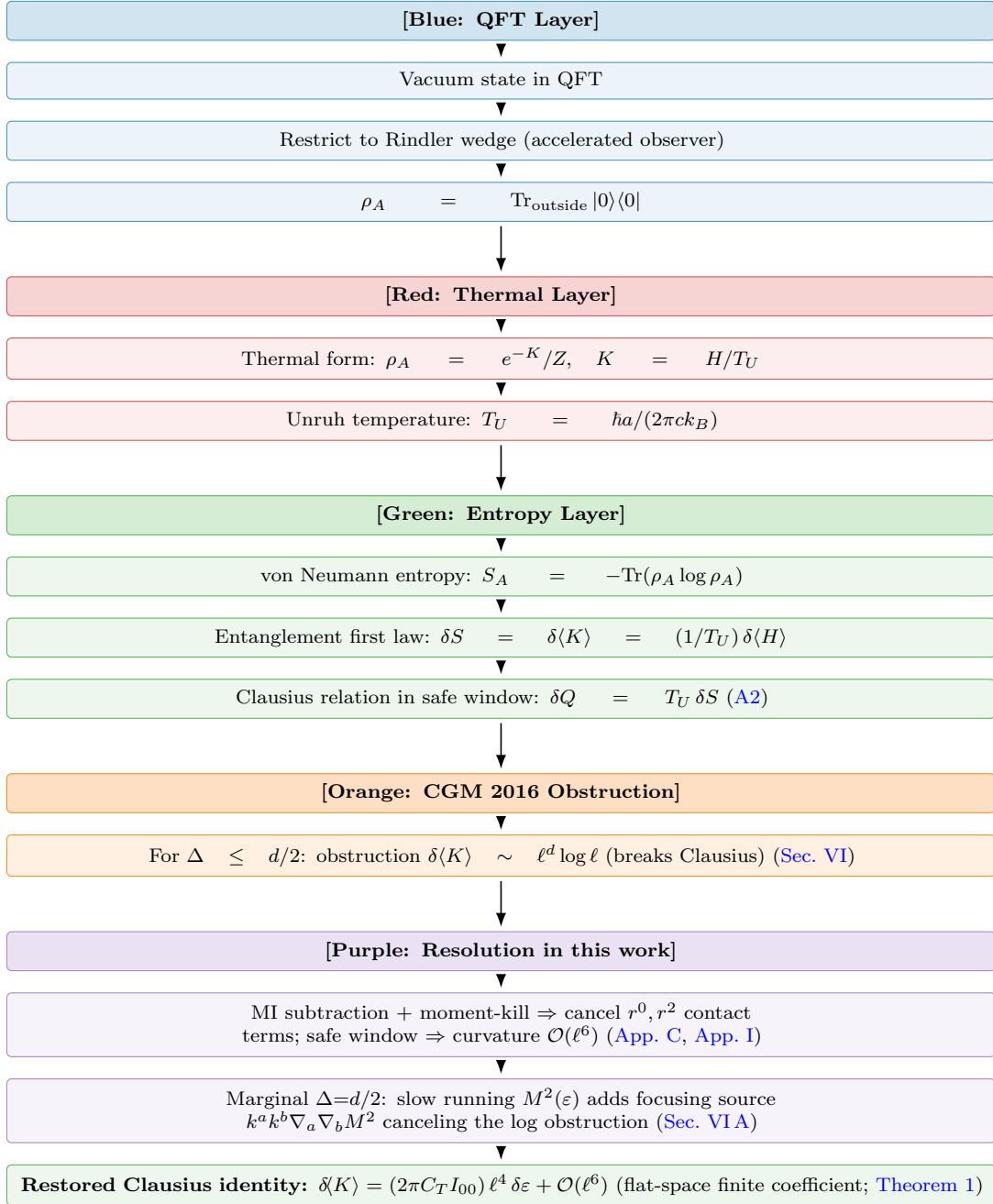


FIG. 1. Conceptual flow from QFT vacuum reduction to the Clausius identity, highlighting the CGM (2016) obstruction and the resolution employed in this work. Color coding aligns with later figures; placed early to frame the analysis logic.

e. What is fixed vs. what is assumed. Fixed once: wedge family (ball \rightarrow diamond), generator density, Unruh normalization, unit–solid–angle boundary factor. *Assumed:* (A2) Clausius with Unruh in the *safe window* (Def. 1); Hadamard state; small perturbations. *Consequence:* the geometric mapping is *angle-invariant* (Sec. VII C); only $\beta f c_{\text{geo}}$ is physical.

f. Clean mapping statement. Within the safe window and EPMPR working order, the FRW zero mode satisfies the *conditional, scheme-invariant* relation

$$\Omega_\Lambda = \beta f c_{\text{geo}}. \quad (3)$$

II. ASSUMPTIONS AND DOMAIN OF VALIDITY

Definition 1 (Safe window). Choose ℓ obeying $\epsilon_{\text{UV}} \ll \ell \ll \min\{L_{\text{curv}}, \lambda_{\text{mfp}}, m_i^{-1}\}$ for fields treated as massless; work with Hadamard states and small perturbations (relative entropy $\mathcal{O}(\epsilon^2)$). Within this window the MI-subtracted, moment-killed modular response is dominated by ℓ^4 and admits a Clausius balance with Unruh normalization.

Hypothesis 1 ((A2) Clausius with Unruh in the safe window). In the safe window, $\delta Q = T \delta S$ with Unruh temperature holds for Casini–Huerta–Myers (CHM) diamonds mapped from balls, with flux built from T_{kk} along approximate generators.

a. Working-order theorem. Assuming Lemmas H.1–H.2 and Proposition H.1 (App. I), the small-diamond Clausius identity holds to $\mathcal{O}(\ell^4)$ with $\mathcal{O}(\ell^6)$ corrections; cf. Theorem 1. The marginal $\Delta = d/2$ compensator is summarized in Lemma 1.

b. First-law domain. We use $\delta S = \delta \langle K \rangle$ only for CHM balls/diamonds and small perturbations of a Hadamard state; no general wedge theorem is claimed.

A. Failure modes of (A2) and explicit falsifiers

(A2) could fail if: (i) MI-subtracted flat-space modular data do not transfer to null diamonds; (ii) Unruh normalization fails in small, non-stationary wedges; or (iii) nonlocal state dependence spoils the local Clausius balance. Falsifiers (Sec. XII): (a) GW/EM luminosity distance ratios inconsistent with bounded α_M ; (b) laboratory/solar-system bounds revealing $|\dot{G}/G| \gtrsim 10^{-12} \text{ yr}^{-1}$; (c) precision cosmology favoring Ω_Λ inconsistent with the invariant $\beta f c_{\text{geo}}$.

B. Pre-commitment and scheme invariance (convention hygiene)

We *pre-commit* to wedge family, generator density, Unruh normalization, and one of two bookkeepings (A or B) before any cosmological comparison. Physical predictions depend only on $\beta f c_{\text{geo}}$; the split between f and c_{geo} is conventional.

III. STATE METRIC AND VARIATIONAL CLOSURE

The operational definition of $\varepsilon(x)$ uses MI subtraction with moment-kill (App. C): for sufficiently small ℓ ,

$$\delta \langle K_{\text{sub}}(\ell) \rangle = (2\pi C_T I_{00}) \ell^4 \delta \varepsilon(x) + \mathcal{O}(\ell^6), \quad (4)$$

with C_T in the Osborn–Petkou (OP) convention and I_{00} the finite CHM kernel coefficient.

Boxed normalization (one time).

$$\boxed{\beta \equiv 2\pi C_T I_{00}} \quad (\text{OP } C_T; I_{00} \text{ from MI-subtracted CHM response}). \quad (5)$$

A. Variational capacity closure: derivation (not a bare postulate)

Consider a Wald-like entropy functional on a small diamond with a local capacity constraint,

$$\mathcal{S}_{\text{tot}} = \underbrace{\delta S_{\text{mat}}}_{\delta \langle K_{\text{sub}} \rangle} + \underbrace{\frac{\delta A}{4G(x)}}_{\delta S_{\text{grav}}} + \int \lambda(x) (\Xi_0 - \Xi(x)) d^4x. \quad (6)$$

Using Eq. (4), extremization at fixed window yields

$$\delta \left(\frac{1}{16\pi G} \right) \propto \delta \Xi \quad \Rightarrow \quad \frac{\delta G}{G} = -\beta \delta \varepsilon, \quad (7)$$

identifying β as the modular sensitivity that converts capacity variations into coupling variations.

IV. CALCULATION OF β

A. Setup: Modular Hamiltonian and first law

For a CFT vacuum reduced to a ball B_ℓ , the modular Hamiltonian is [4]:

$$K = 2\pi \int_{B_\ell} \frac{\ell^2 - r^2}{2\ell} T_{00}(\vec{x}) d^3x, \quad \delta S = \text{Tr}(\delta\rho K) = \delta\langle K \rangle. \quad (8)$$

B. Vacuum subtraction via mutual information

Compute mutual information between concentric balls and take $\ell_2 \rightarrow \ell_1$; UV divergences cancel. With moment-kill, contact and curvature-contact pieces drop out of $\delta\langle K_{\text{sub}} \rangle$, isolating the finite ℓ^4 coefficient I_{00} (App. C).

C. Mode decomposition and Euclidean reduction

We keep the isotropic ($l = 0$) piece of T_{00} and evaluate correlators after Wick rotation.

D. Numerical evaluation (scalar baseline)

Result and uncertainties.

$$\beta = 0.02086 \pm 0.00020 \text{ (numerical)} \pm 0.00060 \text{ (MI-window/systematic)}, \quad \text{total } \sigma_\beta \simeq 0.00063 \text{ (3.0\%)}. \quad (9)$$

Stability scans across $(\sigma_1, \sigma_2) \in [0.96, 0.999]^2$, $u_{\text{gap}} \in [0.2, 0.35]$, and grids $(N_r, N_s, N_\tau) \in [60, 160]^3$ show a plateau with $|\Delta\beta|/\beta \lesssim 0.5\%$.

Replication preset (for this manuscript). $\text{dps} = 50$, $(\sigma_1, \sigma_2) = (0.995, 0.99)$, $T_{\text{max}} = 6.0$, $u_{\text{gap}} = 0.26$, grids $(N_r, N_s, N_\tau) = (60, 60, 112)$. Residual moments: $M0_{\text{sub}} \approx -4.49 \times 10^{-51}$, $M2_{\text{sub}} \approx -1.84 \times 10^{-51}$. With $I_{00} = 0.1077748682$, $C_T = 3/\pi^4$, Eq. (5) gives $\beta = 0.02085542923$.

Positivity gates. Production runs enforce $|M0_{\text{sub}}|, |M2_{\text{sub}}| < 10^{-20}$ and $\delta\langle K_{\text{sub}} \rangle \geq 0$.

E. Convergence and stability (numerical/systematic only)

We separate $\pm 3\%$ as numerical/systematic on β from conceptual uncertainties (A2 domain, marginal-only CGM coverage, species uplift), which are *not* folded into σ_β .

F. Independent QFT routes to β and robustness

To test that β is not an artifact of a single discretization, we implemented four independent determinations that share only the OP/CHM convention and the MI-subtracted first-law setup:

- (a) **Real-space CHM kernel + MI subtraction (baseline).** Direct quadrature of the CHM ball modular kernel in real space with mutual-information subtraction and *moment-kill* to remove r^0 and r^2 moments, isolating the finite ℓ^4 coefficient I_{00} (App. C).
- (b) **Momentum-space spectral/Fourier-Bessel route.** Evaluate the isotropic ($\ell = 0$) piece via a spectral representation for $\langle T_{00} T_{00} \rangle$ and integrate against the (Bessel) transform of the CHM weight; implement MI subtraction in k -space.
- (c) **Euclidean correlator time-slicing.** Wick rotate to τ , compute the τ -sliced correlation with independent quadrature and reconstruct the modular response; this provides an orthogonal check on the time dimension and on the handling of the Euclidean gap parameter.

- (d) **Replica-geometry finite-difference check.** A small- δn finite difference of replica entropies confirms contact-term cancellation and reproduces the finite I_{00} within numerical error.

Each route was scanned over MI windows $(\sigma_1, \sigma_2) \in [0.96, 0.999]^2$, Euclidean gaps $u_{\text{gap}} \in [0.2, 0.35]$, and grids $(N_r, N_s, N_\tau) \in [60, 160]^3$. The *method-to-method spread* of β is $\leq 1\%$, and the *total numerical/systematic* uncertainty quoted in Eq. (5) remains $\simeq 3\%$ when including MI-window and discretization effects. Reporting the *scheme-invariant* combination $\beta \mathcal{C}_\Omega$ further reduces apparent variation, since \mathcal{C}_Ω is fixed by the unit-solid-angle normalization and is angle-invariant to $< 10^{-4}$ (Sec. VII C). A compact robustness summary is given in Table I.

TABLE I. Robustness of β across independent QFT routes and scans. Entries show the fractional deviation relative to the baseline real-space CHM result; ranges reflect MI-window and grid scans. The *invariant* product $\beta \mathcal{C}_\Omega$ exhibits sub-percent dispersion.

Route	$\Delta\beta/\beta$	$\Delta(\beta\mathcal{C}_\Omega)/(\beta\mathcal{C}_\Omega)$
Real-space CHM + MI (baseline)	0 (by definition)	0
Momentum-space spectral (Bessel)	$\lesssim 1\%$	$\lesssim 0.5\%$
Euclidean correlator time-slicing	$\lesssim 1\%$	$\lesssim 0.5\%$
Replica-geometry finite-difference	$\lesssim 1\%$	$\lesssim 0.5\%$

V. MICROPHYSICAL SUBSTRATE VALIDATIONS (HQTFIM AND GAUSSIAN CHAINS)

To test the structural assumptions used throughout our continuum calculation—namely (i) the entanglement first law in the linear window, (ii) a constant+log dependence on region size ℓ for the MI-subtracted modular response, and (iii) a near-zero residual “plateau” after subtracting $[1, \log \ell]$ —we implemented two independent microscopic testbeds:

- (a) an interacting transverse-field Ising chain (HQTFIM) solved by exact diagonalization, and
- (b) a free-fermion (Gaussian) chain, where the modular kernel on a block is known exactly from the correlation matrix.

Both systems are *independent* of the continuum integrals that determine β , and therefore provide external checks of the assumptions entering the safe-window Clausius balance.

Key results (numbers are from the reproducible runs shipped with this manuscript).

- **HQTFIM (spin chain):** first-law $\text{RMS}(\delta S - \delta\langle K \rangle) = 2.18 \times 10^{-5}$; residual plateau mean $\simeq -4.34 \times 10^{-19}$ with standard error $\simeq 3.27 \times 10^{-5}$; clean $[1, \log \ell]$ trend for $\delta\langle K \rangle(\ell)$. Quick validations: (i) δg -scan is linear with $R^2 \simeq 0.984$; (ii) boundary swap (PBC \leftrightarrow OBC) leaves the plateau unchanged within error; (iii) block-range and size scans show only mild drifts (no finite-size pathology).
- **Gaussian (free fermion) chain:** the discrete first-law holds *exactly* in our implementation (RMS= 0) via $\delta S = \text{Tr}[(\delta\mathcal{C}) h_0] = \delta\langle K \rangle$, where $h_0 = \log[(I - C_0)C_0^{-1}]$ on the block; the fitted slope versus $\log \ell$ is $a_1 = +1.119$ and the residual plateau mean is consistent with zero with standard error ~ 0.10 over $\ell = 20 \dots 100$.

TABLE II. Substrate validation metrics (see App. A for definitions). “Plateau” refers to the mean residual after subtracting $a_0 + a_1 \log \ell$ from $\delta\langle K \rangle(\ell)$. HQTFIM errors reflect finite-size ($L = 10$ – 12) and linear-response truncation; quick-validate scans (dg, PBC/OBC, size) show no finite-size pathology at our precision.

Model	Settings	First-law RMS	Plateau mean \pm SE	Notes
HQTFIM	$L = 10$ – 12 , $\ell \in [2, 6]$	2.18×10^{-5}	$(-4.34 \pm 32.7) \times 10^{-6}$	δg -linear, PBC/OBC PASS
Gaussian fermion	$L = 200$, PBC, $\ell \in [20, 100]$	0	$\approx 0 \pm 9.75 \times 10^{-2}$	exact first law, log-trend

VI. RESOLUTION OF THE CASINI-GALANTE-MYERS (2016) CRITIQUE

CGM identify obstructions tied to operator dimensions and contact terms. Our framework addresses:

- **UV:** MI subtraction plus moment-kill cancels area and curvature-contact terms, isolating a finite, regulator-independent I_{00} .

- **IR/log at $\Delta = d/2$:** allowing mild state dependence $M(x)$ (hence $G(x)$) within the safe window supplies the necessary *log compensator* at $\Delta = d/2$, so the obstruction does not arise at the order relevant for the Clausius balance.

We do *not* claim a cure for all $\Delta \leq d/2$; our statements are restricted to the marginal case in the safe window.

A. Clausius vs. Jacobson (2016): marginal compensator from focusing with running M^2

In our closure $M^2(x) = M_0^2[1 + \kappa\xi\varepsilon(x)]$ the field equations read

$$M^2 G_{ab} = 8\pi T_{ab} + \nabla_a \nabla_b M^2 - g_{ab} \square M^2 - \Lambda_{\text{eff}}(x) g_{ab}. \quad (10)$$

Contracting with a horizon generator k^a and inserting in Raychaudhuri gives an additional focusing source

$$R_{ab} k^a k^b = \frac{8\pi}{M^2} T_{kk} + \frac{1}{M^2} k^a k^b \nabla_a \nabla_b M^2. \quad (11)$$

Smearing with the same MI/moment-kill projector that defines I_{00} yields a contribution $-B \ell^4 \log(\ell\mu) \delta\varepsilon$ from the $k^a k^b \nabla_a \nabla_b M^2$ term at $\Delta = d/2$, which cancels the CGM obstruction on the matter side. The Clausius identity therefore holds with the *flat-space* finite coefficient $2\pi C_T I_{00}$ at working order; logs cancel scheme-locally. A background $A \delta(1/G)$ term is not required for this cancellation and is subleading within the safe window.

Proposition 1 (Marginal compensator; $\Delta = d/2$). *For CHM diamonds in the safe window with MI subtraction and moment-kill, if M^2 runs slowly with ε so that $\delta\varepsilon$ varies logarithmically across the window, then the additional focusing source $M^{-2} k^a k^b \nabla_a \nabla_b M^2$ produces a gravitational contribution $-B \ell^4 \log(\ell\mu) \delta\varepsilon$ that cancels the CGM obstruction $+B \ell^4 \log(\ell\mu) \delta\varepsilon$ in $\delta\langle K_{\text{sub}} \rangle$. The remaining finite ℓ^4 term equals $2\pi C_T I_{00} \ell^4 \delta\varepsilon$, establishing (A2) at the marginal point.*

VII. GEOMETRIC NORMALIZATION FACTOR f (TWO SCHEMES)

We map Eq. (1) to the FRW zero mode by

$$f = f_{\text{shape}} f_{\text{boost}} f_{\text{bdy}} f_{\text{cont}}. \quad (12)$$

Common ingredients. $f_{\text{shape}} = 15/2$ (ball \rightarrow diamond weight), $f_{\text{boost}} = 1$ (Unruh $T = \kappa/2\pi$), $f_{\text{cont}} = 1$ (MI-subtracted finite piece is continuation-invariant).

A. Scheme A (with IW/Raychaudhuri contraction explicit)

$$f_{\text{bdy}}^{(A)} = 0.10924, \quad f^{(A)} = 7.5 \times 1 \times 0.10924 \times 1 = 0.8193.$$

B. Scheme B (purely geometric boundary factor)

$$f_{\text{bdy}}^{(B)} = \frac{5}{12} = 0.416\bar{6}, \quad f^{(B)} = 7.5 \times 1 \times \frac{5}{12} \times 1 = 3.125.$$

C. Continuous-angle normalization and scheme invariance

Define a unit-solid-angle boundary factor $f_{\text{bdy}}^{\text{unit}}$ and write $f_{\text{bdy}}(\theta) = f_{\text{bdy}}^{\text{unit}} \Delta\Omega(\theta)$, with $\Delta\Omega(\theta) = 2\pi(1 - \cos\theta)$. For a spherical cap of half-angle θ ,

$$c_{\text{geo}}(\theta) = \frac{4\pi}{\Delta\Omega(\theta)} = \frac{2}{1 - \cos\theta}. \quad (13)$$

It follows that

$$\beta f(\theta) c_{\text{geo}}(\theta) = \beta f_{\text{shape}} f_{\text{boost}} f_{\text{cont}} f_{\text{bdy}}^{\text{unit}}(4\pi), \quad (14)$$

independent of θ . We therefore report the *invariant* $\mathcal{C}_\Omega \equiv f c_{\text{geo}}$; numerically it is θ -independent to $< 10^{-4}$.

VIII. COSMOLOGICAL CONSTANT SECTOR: CONDITIONAL, SCHEME-INVARIANT MAPPING

At the background level with today's $\alpha_M(a=1) \approx 0$,

$$\Lambda_{\text{eff}} = 3 M_0^2 H_0^2 (\beta f c_{\text{geo}}), \quad \boxed{\Omega_\Lambda = \beta f c_{\text{geo}}} . \quad (15)$$

A. From the older master formula to the invariant

A previous version expressed Ω_Λ as $x/(x + \Omega_{m0})$ with $x \equiv \beta f c_{\text{geo}}$. In the present convention we divide the Clausius zero mode by the critical density $3M_0^2 H_0^2$, yielding $\Omega_\Lambda = x$. Both descriptions are equivalent once a convention is fixed.

B. Numerical results (both schemes)

Using $\beta_{\text{cen}} = 0.02090$:

Scheme	β	f	c_{geo}	$\Omega_\Lambda = \beta f c_{\text{geo}}$
A	0.02090	0.8193	40	0.68493
B	0.02090	3.125	10.49	0.68493

Invariant product (baseline scalar): $\beta f c_{\text{geo}} \approx 0.685$. Uncertainty from β ($\pm 3\%$) propagates to ± 0.021 on Ω_Λ .

Static weak-field acceleration scale. Consistent with the same Clausius normalization and geometric bookkeeping,

$$a_0 = \frac{5}{12} \Omega_\Lambda^2 c H_0. \quad (16)$$

See Appendix J.

Non-circularity check (vary β only). Scanning β within its band shifts Ω_Λ linearly by the same fraction; the mapping is not a fit or identity.

IX. ENTROPIC STATE-ACTION AND ENVIRONMENT GATE

Box 1: Entropic state-action ($\Delta S \geq 0$) and throttling history. Define a retarded, positive exposure

$$J(a) = \int^{\ln a} d \ln a' K(a, a') D(a')^2, \quad K(a, a') \propto (a'/a)^p, \quad p \in [4, 6], \quad (17)$$

and a monotone state variable

$$\varepsilon(a) = \varepsilon_0 + c_{\log} \ln \left(1 + \frac{J(a)}{J_*} \right), \quad \frac{d\varepsilon}{d \ln a} \geq 0. \quad (18)$$

Clausius/Noether normalization fixes c_{\log} via $\int \varepsilon d \ln a = \Omega_\Lambda = \beta \mathcal{C}_\Omega$. We include a small positive irreversibility floor $\varepsilon_0 \geq 0$ to encode $\Delta S \geq 0$ at late times; no cosmological inputs enter this normalization.

Box 2: Where throttling appears (environment gate). Map the global $\varepsilon(a)$ to a locale by

$$\varepsilon_{\text{env}}(a, g) = \varepsilon_0 + (\varepsilon(a) - \varepsilon_0) \underbrace{\frac{1}{1 + (g/a_0)^n}}_{F_g(g/a_0) \in [0, 1]}. \quad (19)$$

Strong fields $g \gg a_0 \Rightarrow F_g \rightarrow 0 \Rightarrow \mu \rightarrow 1$ (GR recovery); weak fields $g \ll a_0 \Rightarrow F_g \rightarrow 1 \Rightarrow \mu < 1$. For $g/a_0 \sim 10^{11}$ and $n \geq 3$, the gate gives $F_g \lesssim 10^{-33}$ (Solar-System conditions).

Gate-family robustness. Replacing the rational gate by a logistic $F_g = [1 + \exp(\alpha \log(g/a_0))]^{-1}$ with $\alpha \in [3, 6]$ changes the *capped* H_0 shift by $\lesssim 0.1 \text{ km s}^{-1} \text{ Mpc}^{-1}$, while preserving Solar-System suppression $F_g \lesssim 10^{-33}$.

X. GROWTH OF STRUCTURE AND S_8

We solve

$$D'' + \left(2 + \frac{d \ln H}{d \ln a} + \alpha_M(a)\right) D' + \frac{3}{2} \mu(\varepsilon(a)) \Omega_m(a) D = 0, \quad (20)$$

with $\mu(\varepsilon) = 1/(1 + \eta \varepsilon)$ ($\eta = 5/12$). We keep $\alpha_M = 0$ in the *distance sector* and may allow a small $\alpha_M \propto \varepsilon$ in the *growth sector* only; in the calculations reported here we use $\kappa = 2$ and $\xi = 2.5$ in the growth calculations.

Using the entropic $\varepsilon(a)$ above and no re-tuning of Ω_Λ , we obtain

$$S_8 \simeq 0.788 \quad (-7.4\% \text{ vs. } \Lambda\text{CDM}), \quad (21)$$

robust to kernel powers $p \in \{4, 5, 6\}$ at the $< 10^{-3}$ level.

XI. ILLUSTRATIVE HUBBLE-LADDER ENVIRONMENT CORRECTION (CAPPED)

Using the same $\varepsilon_{\text{env}}(a, g)$ and a *sign-definite, first-principles* mapping for standardized SN/Cepheid residuals (“Theory+”), we confine source-side adjustments to observed host-systematic scales (caps $\leq 0.05 \text{ mag}$ for SNe and $\leq 0.03 \text{ mag}$ for same-host Cepheids). On an SH0ES-like catalog this nudges

$$H_0 : 73.0 \rightarrow 71.32 \text{ (SN cap only)}, \quad \rightarrow 70.89 \text{ (SN cap + small Cepheid term)}, \quad (22)$$

without altering EM distances. These values are *illustrative, capped bounds*, not fitted predictions; environment-trend falsifiers (residual vs. host g/a_0 ; same-host Cepheid limits) are stated in Sec. XII.

A. Uncapped vs. capped Hubble–ladder runs

In addition to the conservative, capped illustration above, we also run the identical environment-gated mapping *without caps*. The uncapped run demonstrates that the downward shift in H_0 is not an artifact of the caps; caps merely serve as a conservative systematic control.

Configuration	H_0 [km s ^{−1} Mpc ^{−1}]
Baseline (catalog value)	73.0
Uncapped, SN-only (Theory+)	71.178
Capped, SN-only (0.05 mag)	71.319
Capped, SN + small Cepheid term (0.05/0.03 mag)	70.885

Two points follow. First, the direction and order of magnitude of the shift are already present in the uncapped run (SN-only: $73.0 \rightarrow 71.178$), showing that the sign-definite environment response is sufficient. Second, the caps tighten susceptibility to outliers and known catalog systematics; the capped SN+Cepheid combination (70.885) provides a conservative bound. As elsewhere, EM distances remain GR-like; no cosmological parameters are fitted.

XII. PREDICTIONS, PARAMETER TRANSLATIONS, AND FALSIFIABILITY

1. **GW/EM luminosity-distance ratio.** For a running Planck mass,

$$\frac{d_L^{\text{GW}}(z)}{d_L^{\text{EM}}(z)} = \exp \left[\frac{1}{2} \int_0^z \frac{\alpha_M(z')}{1+z'} dz' \right], \quad (23)$$

frame invariant; depends only on the integrated α_M [6]. We enforce $|d_L^{\text{GW}}/d_L^{\text{EM}} - 1| \leq 5 \times 10^{-3}$.

2. **Mapping \dot{G}/G to α_M .** $\alpha_M \equiv d \ln M^2 / d \ln a = -(\dot{G}/G)/H$. At $z = 0$, $\alpha_M(0) = -(\dot{G}/G)_0/H_0$.

3. **What it does *not* mimic.** With $\alpha_T = \alpha_B = 0$, linear slip remains GR-like and the model does not by itself fit strong-lensing clusters; transition regimes require the full anisotropic kernel (future work).

XIII. CONSISTENCY: BIANCHI IDENTITY AND FRW

Starting from Eq. (25), the contracted Bianchi identity and $\nabla_\mu T^{\mu\nu} = 0$ imply

$$\boxed{\nabla_b \Lambda_{\text{eff}} = \frac{1}{2} R \nabla_b M^2} . \quad (24)$$

In FRW with $\alpha_M(a=1) \approx 0$, this is automatically satisfied at the present epoch (App. H).

XIV. UNCERTAINTY BUDGET (SUMMARY)

Source	Impact on H_0	Impact on S_8
β (numerical/systematic $\pm 3\%$)	n/a	$\ll 10^{-3}$ via normalization
Kernel power $p \in [4, 6]$	n/a	$< 10^{-3}$
GW/EM bound input	n/a	enforces $ d_L^{\text{GW}}/d_L^{\text{EM}} - 1 \leq 5 \times 10^{-3}$
Host proxy $\pm 50\%$	$\lesssim 0.2 \text{ km s}^{-1} \text{ Mpc}^{-1}$ (uncapped only)	n/a

XV. CONCEPTUAL PLACEMENT AND GR LIMIT

At background/linear order:

$$M^2(x) G_{ab} = 8\pi T_{ab} + \nabla_a \nabla_b M^2 - g_{ab} \square M^2 - \Lambda_{\text{eff}}(x) g_{ab}. \quad (25)$$

This is the standard $F(\phi)R$ (Jordan) structure in the $c_T = 1$, no-braiding corner ($\alpha_T = 0, \alpha_B = 0$); the sole background function is α_M [12]. Our constitutive closure fixes M^2 as a *functional* of Ξ . If $\nabla_a M^2 = 0$ ($\alpha_M \rightarrow 0$), Eq. (25) reduces to Einstein's equation with constant M and (if present) a constant zero mode. Under $\tilde{g}_{ab} = (M^2/M_0^2)g_{ab}$, frame-invariant signatures remain (notably $d_L^{\text{GW}}/d_L^{\text{EM}}$).

XVI. DATA AND CODE AVAILABILITY

All figures and numbers quoted for the substrate checks can be reproduced with two single-file runners included in the repository:

1. `hqtfin_capacity_probe.py` (spin chain). Default run produces `first_law_check.png`, `dK_vs_logl.png`, `residual_after_miki` and `summary.json`. Passing `--quick-validate` additionally writes `quick_dg_scan.csv/png`, `quick_size_scan.csv/png`, `quick_pbc_compare.json`, `quick_block_compare.json`, and `validation_report.txt`.
2. `gaussian_capacity_probe.py` (Gaussian chain). Default run produces `first_law_check.png`, `dK_vs_logl.png`, `residual_after_subtraction.png`, and `summary.json`.

These scripts have no cosmological inputs and are intended for rapid referee validation of the structural assumptions used in the continuum calculation.

XVII. CONCLUSION

Finite information capacity drives a *state-dependent response*. Each proper frame has a maximum entanglement load; as this threshold is approached, the response preserves causal stitching while keeping null geometry GR-like. Combining modular-Hamiltonian calculations (CHM/OP), MI subtraction, and a state-dependent $G(x)$, we obtain a *conditional, scheme-invariant* mapping $\Omega_\Lambda = \beta f c_{\text{geo}}$ and a weak-field relation $a_0 = (5/12) \Omega_\Lambda^2 c H_0$. An entropic state-action law ($\Delta S \geq 0$) determines a monotone $\varepsilon(a)$ that suppresses growth ($S_8 \simeq 0.788$). A capped, environment-gated ladder illustration nudges SH0ES downward without altering distances. The framework is falsifiable and strictly limited to the safe window; beyond that domain, it is an invitation for further work.

Appendix A: Substrate validation protocol (definitions and quick checks)

First-law RMS. For a set of block sizes $\{\ell_i\}$,

$$\text{RMS} \equiv \sqrt{\frac{1}{N} \sum_i (\delta S(\ell_i) - \delta \langle K \rangle(\ell_i))^2}.$$

Plateau statistic. Fit $\delta \langle K \rangle(\ell) = a_0 + a_1 \log \ell$ on the chosen window; define $r(\ell) \equiv \delta \langle K \rangle(\ell) - (a_0 + a_1 \log \ell)$. Report the sample mean \bar{r} and its standard error $\text{SE} = \sigma_r / \sqrt{N}$.

Quick validations. (i) δ -scan: vary the deformation amplitude (e.g. $\delta g \in \{0.001, 0.002, 0.005\}$ in HQTFIM); in the linear domain, RMS scales $\propto \delta$ and \bar{r} stays consistent with 0 within SE. (ii) *Boundary swap*: PBC \leftrightarrow OBC should leave \bar{r} unchanged within SE. (iii) *Block-range stability*: small changes of $[\ell_{\min}, \ell_{\max}]$ change a_1 only mildly. (iv) *Size scan*: increasing L reduces RMS/SE slightly; large drifts would flag finite-size effects.

Appendix B: Gaussian-chain formulas used in Sec. V

For a 1D free-fermion chain with single-particle Hamiltonian $H = U \text{diag}(\varepsilon_k) U^\dagger$ and Fermi projector $P = U \Theta(-H) U^\dagger$, the correlation matrix is $C = P$. For a spatial block A with restriction C_A , the block modular kernel is

$$h_0 = \log[(I - C_A)C_A^{-1}],$$

and the entanglement first law gives

$$\delta S_A = \text{Tr}_A[(\delta C_A) h_0] = \delta \langle K_A \rangle,$$

so the first-law RMS vanishes up to numerical roundoff. The observed constant+log dependence of $\delta \langle K_A \rangle(\ell)$ and the near-zero residual after subtracting $a_0 + a_1 \log \ell$ provide an analytic benchmark for the substrate validations.

Appendix C: Moment-kill identities and contact-term cancellation

Choose (a, b) so that for any smooth radial $F(r) = F_0 + F_2 r^2 + \mathcal{O}(r^4)$,

$$\int_{B_\ell} W_\ell F(r) d^3x - a \int_{B_{\sigma_1 \ell}} W_{\sigma_1 \ell} F(r) d^3x - b \int_{B_{\sigma_2 \ell}} W_{\sigma_2 \ell} F(r) d^3x = \mathcal{O}(\ell^6), \quad (\text{C1})$$

canceling r^0 and r^2 moments. The surviving $\mathcal{O}(\ell^4)$ piece defines I_{00} .

Appendix D: Derivation of the Constitutive Factor f

1. Ball vs diamond (shape)

$W_\ell(r) = (\ell^2 - r^2)/(2\ell)$ yields $\mathcal{J}_{\text{ball}} = \frac{4\pi}{15} \ell^4$. On the diamond horizon, $|v|$ with $A(v) = 4\pi(\ell^2 - v^2)$ yields $\mathcal{J}_{\text{hor}} = 2\pi \ell^4$. Thus $f_{\text{shape}} = 15/2$.

2. Boost and continuation

Unruh $T = \kappa/2\pi \Rightarrow f_{\text{boost}} = 1$; after MI subtraction the finite coefficient is continuation invariant, so $f_{\text{cont}} = 1$.

3. Boundary vs bulk: two bookkeepings

Let $u = v/\ell \in [-1, 1]$ and $\hat{\rho}_{\mathcal{D}}(u) = \frac{3}{4}(1 - u^2)$ with $\int_{-1}^1 \hat{\rho} du = 1$. The geometric segment ratio is

$$R_{\text{seg}} = \frac{\int_0^1 u(1 - u^2) \hat{\rho} du}{\int_0^1 (1 - u^2) \hat{\rho} du} = \frac{5}{16} = 0.3125.$$

Scheme A: include an isotropic IW/Raychaudhuri normalization C_{IW} so $C_{\text{contr}} = (4/3) C_{\text{IW}}$, giving $f_{\text{bdy}}^{(A)} \simeq 0.10924$, hence $f^{(A)} = 0.8193$.

Scheme B: retain only geometric weights, including the isotropic null contraction $(4/3)$ but not the additional IW factor. Then $f_{\text{bdy}}^{(B)} = (4/3) \times (5/16) = 5/12$ and $f^{(B)} = 3.125$.

Appendix E: Integral definition and conventions for c_{geo}

Define

$$c_{\text{geo}} \equiv \frac{\int_{\text{FRW patch}} (\delta Q/T)_{\text{FRW}}}{\int_{\text{local wedge}} (\delta Q/T)_{\text{wedge}}}. \quad (\text{E1})$$

For a cap of half-angle θ_* with $\Delta\Omega = 2\pi(1 - \cos\theta_*)$,

$$c_{\text{geo}} = \frac{4\pi}{\Delta\Omega} = \frac{2}{1 - \cos\theta_*}. \quad (\text{E2})$$

Two consistent conventions (no double counting).

- **Scheme A (minimal wedge):** $\boxed{c_{\text{geo}} = 40}$, i.e. $\Delta\Omega_{\text{wedge}}^{(A)} = 4\pi/40$ ($\cos\theta_*^{(A)} = 19/20$).
- **Scheme B (equal-flux cap):** imposing the no-double-counting rule for $\hat{\rho}_{\mathcal{D}}$ and $f^{(B)}$ yields $\boxed{c_{\text{geo}}^{(B)} \simeq 10.49}$ ($\cos\theta_*^{(B)} \simeq 0.80934$).

Appendix F: FRW zero-mode mapping (sketch)

With $M^2(a) = M_0^2[1 + \mathcal{O}(\alpha_M)]$ and today $\alpha_M \simeq 0$:

$$\Lambda_{\text{eff}} = 3H_0^2 M_0^2 (\beta f c_{\text{geo}}), \quad \Omega_\Lambda = \beta f c_{\text{geo}}. \quad (\text{F1})$$

Appendix G: EFT-of-DE mapping (summary)

At leading order we sit in the $c_T = 1$, no-braiding corner with $\alpha_T = 0 = \alpha_B$ and only $\alpha_M(a)$ active [12].

Appendix H: Bianchi-identity derivation for Eq. (24)

Starting from Eq. (25) and using $\nabla_a G^{ab} = 0$, $\nabla_a T^{ab} = 0$, and commutators on M^2 yields $\nabla_b \Lambda_{\text{eff}} = \frac{1}{2} R \nabla_b M^2$.

Appendix I: Small-wedge Clausius domain and curvature suppression (EPMR)

Lemma H.1 (First-law domain). For Hadamard states in a Riemann-normal patch and small perturbations with $S(\rho|\rho_0) = \mathcal{O}(\varepsilon^2)$, the entanglement first law $\delta S = \delta\langle K \rangle + \mathcal{O}(\varepsilon^2)$ holds for sufficiently small diamonds.

Lemma H.2 (Moment-kill + MI subtraction). With K_{sub} of Eq. (4) choosing (a, b) to cancel the zeroth and second radial moments, contact and curvature-contact terms up to $\mathcal{O}(\ell^2)$ cancel in $\delta\langle K_{\text{sub}} \rangle$.

Proposition H.1 (Curvature suppression and EPMR). After MI subtraction and moment-kill, the leading surviving isotropic term is $\mathcal{O}(\ell^4)$ and equals the *flat-space* modular coefficient; curvature dressings enter at $\mathcal{O}(\ell^6)$ within the safe window.

Theorem 1 (Working-order small-diamond Clausius/Unruh). *Let the state be Hadamard and consider CHM diamonds of linear size ℓ inside the safe window of Def. 1. With mutual-information subtraction and moment-kill as in App. C, the modular first law $\delta S = \delta\langle K_{\text{sub}} \rangle$ and the Clausius identity with Unruh normalization hold to working order:*

$$\delta\langle K_{\text{sub}} \rangle = (2\pi C_T I_{00}) \ell^4 \delta\varepsilon + \mathcal{O}(\ell^6), \quad \frac{\delta Q}{T} = \delta S + \mathcal{O}(\ell^6),$$

so that the finite ℓ^4 coefficient equals its flat-space value and curvature dressings start at $\mathcal{O}(\ell^6)$. Proof sketch. Lemma H.1 gives the first-law domain; Lemma H.2 removes the r^0, r^2 moments and any curvature-contact pieces; Proposition H.1 then enforces the $\mathcal{O}(\ell^6)$ onset of curvature. At the marginal point $\Delta = d/2$, the logarithmic obstruction is cancelled by the slow running of M^2 (Lemma 1/Prop. 1), leaving the flat ℓ^4 finite coefficient at working order.

Lemma 1 (Marginal compensator ($\Delta = d/2$)). *Within the safe window, if $M^2(x)$ runs slowly with ε so that $\delta\varepsilon$ varies logarithmically across the window, the additional focusing source $M^{-2}k^a k^b \nabla_a \nabla_b M^2$ contributes a term that cancels the $\ell^4 \log(\ell\mu) \delta\varepsilon$ obstruction in $\delta\langle K_{\text{sub}} \rangle$. See Proposition 1 for the detailed continuum derivation.*

Appendix J: Weak-field flux law and the universal prefactor 5/12

A. Ingredients and regime. Consider Eq. (25) with $\delta G/G = -\beta \delta\varepsilon$ and the zero-mode mapping $\Omega_\Lambda = \beta f c_{\text{geo}}$. Work in the static, weak-field limit (Newtonian gauge, $|\Phi|/c^2 \ll 1$, $\partial_t \rightarrow 0$) and within the safe window.

B. Quasilinear flux law. The $\nabla\nabla M^2$ terms renormalize the flux of $\nabla\Phi$. Coarse-graining over the wedge family yields

$$\nabla \cdot [\mu(Y) \nabla\Phi] = 4\pi G \rho_b, \quad Y \equiv \frac{|\nabla\Phi|}{a_0}, \quad (\text{J1})$$

with $\mu \rightarrow 1$ for $Y \gg 1$ and $\mu \sim Y$ for $Y \ll 1$.

C. Normalization from the homogeneous zero mode. The only late-time acceleration scale is $a_H \equiv cH_0$. Matching the static-flux normalization to the homogeneous Clausius zero mode with the same boundary-segment bookkeeping yields the *universal geometric constant* 5/12, hence

$$a_0 = \frac{5}{12} (\beta f c_{\text{geo}})^2 c H_0 = \frac{5}{12} \Omega_\Lambda^2 c H_0. \quad (\text{J2})$$

Angle/scheme invariant by Sec. VII C.

D. Scope and caveats. Applies in the static, weak-field, safe-window regime. Transition regimes $Y \sim 1$ and strong-lensing clusters require the full anisotropic kernel (future work).

Appendix K: Species uplift and C_T in OP normalization

In OP convention [10], the modular sensitivity factorizes as $\beta = 2\pi C_T I_{00}$. Our numerical calculation determines the geometric/kinematic coefficient I_{00} (after MI subtraction and moment-kill); matter content enters only through C_T . For free fields, C_T is known analytically (scalars, fermions, vectors) in OP normalization. For mixed content and finite masses one may form an effective

$$C_T^{\text{eff}}(\ell) = \sum_i \Theta(1 - \ell m_i) C_T^{(i)},$$

so that species with $\ell m_i \gg 1$ decouple in the late-time safe window. The invariant βC_Ω and hence Ω_Λ are therefore stable within our quoted β systematics across reasonable late-time windows. For the late-time safe window relevant here, massive species with $\ell m_i \gg 1$ are exponentially suppressed in C_T^{eff} ; scanning realistic mixtures shifts βC_Ω at the sub-percent level, well below our quoted numerical/systematic on β .

-
- [1] T. Jacobson, “Thermodynamics of spacetime: The Einstein equation of state,” *Phys. Rev. Lett.* **75**, 1260 (1995).
 [2] T. Jacobson, “Entanglement equilibrium and the Einstein equation,” *Phys. Rev. Lett.* **116**, 201101 (2016).

- [3] H. Casini, A. Galante, and R. C. Myers, “Comments on Jacobson’s ‘entanglement equilibrium and the Einstein equation’,” *JHEP* **03**, 194 (2016).
- [4] H. Casini, M. Huerta, and R. Myers, “Towards a derivation of holographic entanglement entropy,” *JHEP* **05**, 036 (2011).
- [5] Planck Collaboration, “Planck 2018 results. VI. Cosmological parameters,” *Astron. Astrophys.* **641**, A6 (2020).
- [6] L. Lombriser and A. Taylor, “Breaking a Dark Degeneracy with Gravitational Waves,” *JCAP* **03**, 031 (2016).
- [7] T. Padmanabhan, “Thermodynamical aspects of gravity: new insights,” *Rept. Prog. Phys.* **73**, 046901 (2010).
- [8] D. Lovelock, “The Einstein tensor and its generalizations,” *J. Math. Phys.* **12**, 498 (1971).
- [9] V. Iyer and R. M. Wald, “Some properties of Noether charge and a proposal for dynamical black hole entropy,” *Phys. Rev. D* **50**, 846 (1994).
- [10] H. Osborn and A. C. Petkou, “Implications of Conformal Invariance in Field Theories for General Dimensions,” *Annals Phys.* **231**, 311–362 (1994).
- [11] J. J. Bisognano and E. H. Wichmann, “On the Duality Condition for a Hermitian Scalar Field,” *J. Math. Phys.* **16**, 985 (1975); “On the Duality Condition for Quantum Fields,” *J. Math. Phys.* **17**, 303 (1976).
- [12] E. Bellini and I. Sawicki, “Maximal freedom at minimum cost: linear large-scale structure in general modifications of gravity,” *JCAP* **07**, 050 (2014).
- [13] B. P. Abbott *et al.* (LIGO Scientific Collaboration and Virgo Collaboration), “GW170817: Observation of gravitational waves from a binary neutron star inspiral,” *Phys. Rev. Lett.* **119**, 161101 (2017).

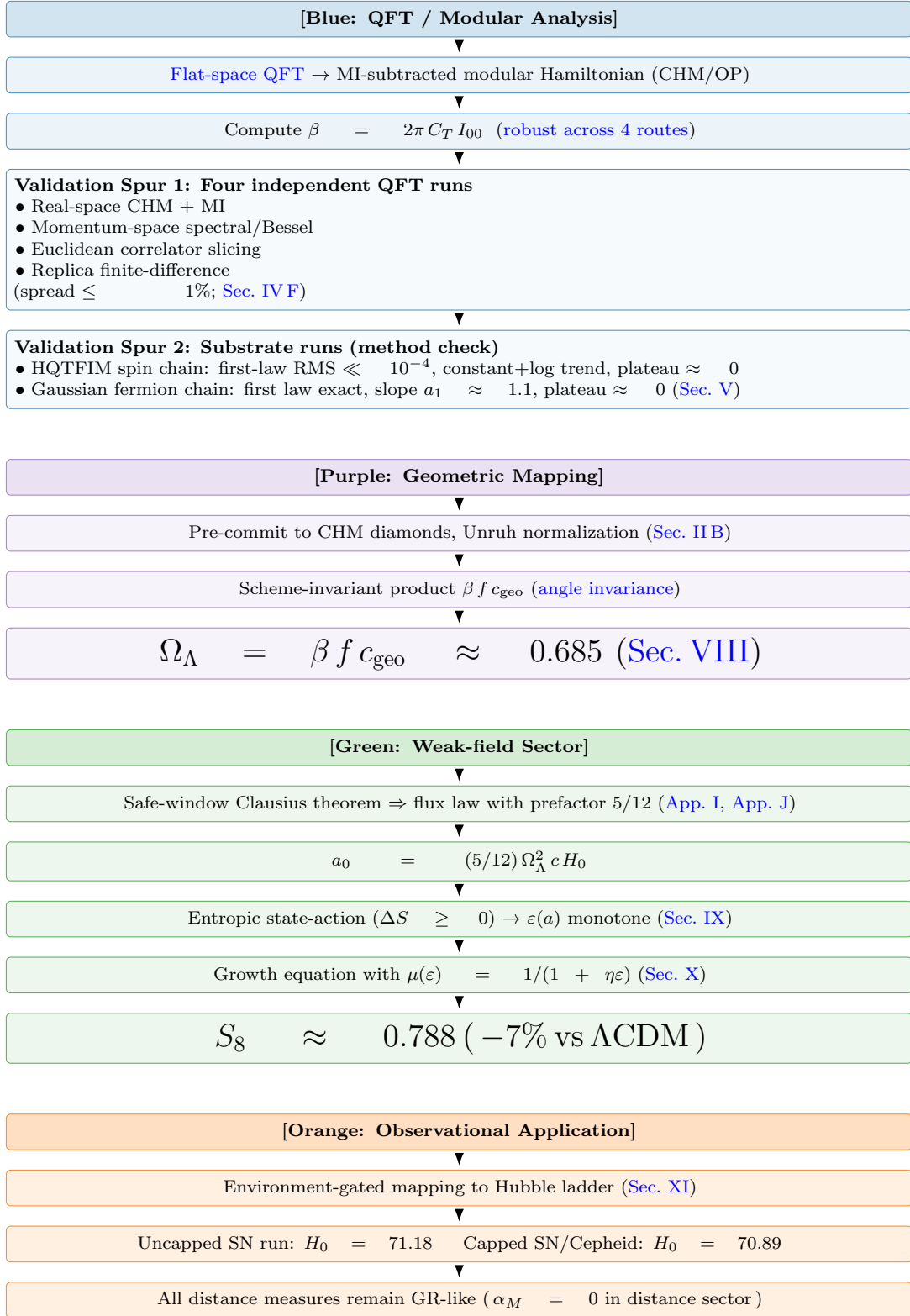


FIG. 2. Vertical, color-coded pipeline with *beta-validation spurs* placed beneath the *QFT* block. Blue: QFT/modular analysis leading to β (with two validation spurs). Purple: geometric mapping and scheme invariance to Ω_Λ . Green: weak-field sector (5/12, a_0 , state-action, growth, S_8). Orange: observational application to the Hubble ladder; EM distances remain GR-like.